2019 American Control Conference (ACC)
Philadelphia, PA, USA, July 10-12, 2019

Optimal actuator shape design with input and state constraints for a wafer heating application

D.W.M. Veldman[1], R.H.B. Fey[1], H.J. Zwart[1,2], M.M.J. van de Wal[3], J.D.B.J. van den Boom[3], H. Nijmeijer[1]

Abstract— **Thermal actuation can reduce deterioration of the imaging quality due to wafer heating. Because the placement of thermal actuators is critical for the performance of the resulting control system, a method to aid the design of an actuator layout is developed. Optimal actuator shapes are computed as the solution of an optimization problem that involves input and state constraints. The resulting actuator shapes have a clear physical interpretation for the next-generation wafer scanners and numerical results seem to indicate that the designed actuator shapes might be unique.**

I. INTRODUCTION

A crucial step in the production of Integrated Circuits (ICs) is the projection of the pattern of electronic connections on a silicon wafer coated with a photoresist. The light source used to project the pattern on the wafer causes the wafer to heat up and expand, which leads to a deteriorated imaging quality. With the critical dimensions of the projected pattern approaching the subnanometer range, wafer heating has become a determining factor for the quality of the produced ICs (see e.g. [1], [2], [3]).

The effect of wafer heating can potentially be mitigated by applying a thermal actuation heat load to the wafer. Such actuation heat load will be generated by thermal actuators that are placed above the wafer. Clearly, the placement of these actuators is critical for the performance of the resulting control system. Therefore, the design of such a thermal actuator layout is an important (but nontrivial) task. In particular, such a design should be able to reduce the deformations in the wafer below a certain treshold by using only a small amount of heating power. Furthermore, many types of actuators can only heat or only cool. Therefore, deciding which areas of the wafer should be heated and which areas of the wafer should be cooled is an important design decision.

The design of such an actuator layout can be considered as an input selection problem for which many methods have been developed (see e.g. [4], [5]). Because information about the heat load generated by the expose light is available, methods that can use this information seem most natural for this problem. Such methods have been proposed by Al-Sulaiman and Zaman [6] and Cao, Biss, and Perkins [7]. For every input set, both methods evaluate a quadratic cost function similar to the one used in the Linear Quadratic Tracking (LQT) (see e.g. [8]). An advantage of this approach is that input constraints can be included. However, the application of these methods to the wafer heating application leads to two main problems.

The first problem is that the physics of the problem is essentially governed by Partial Differential Equations (PDEs) which means there is a very large number of possible actuator layouts, even after spatial discretization by, for example, the Finite Element (FE) method. Therefore, evaluating the cost function for every input set is computationally intractable. Some recent publications show that evaluating the cost function for every input set is not necessary when the problem formulation is changed. For example, Boulanger and Trautman [9] have developed a method to place point actuators to minimize an LQT cost function for the one-dimensional Korteweg-de Vries-Burgers equation by solving a system of nonlinear equations using Newton iteration. Also the work of Privat, Trélat, and Zuazua [10] and Kalise, Kunisch, and Sturm [11] is worth mentioning in this context. In both papers, an optimal actuation restriction problem is studied, i.e. the question "if actuation can only be applied in a certain fraction of the considered spatial domain, actuation in which area of the domain is most effective?" is answered. In [10], an analytic solution for one-dimensional parabolic equations is derived and in [11], a gradient-based optimization algorithm is proposed and applied to two-dimensional problems. The approach in [10] can also be applied to the optimal actuator shape design problem considered in this paper. In contrast to the optimal actuation restriction problem, actuation can now be applied in the whole design domain but is required to have a fixed shape of which the intensity varies over time. This problem can also be considered as a combined plant and control design problem (see e.g. [12]), in which the shape of the actuation heat load is considered as part of the plant and the intensity as a control input. The optimal actuator shape design problem is considered in this paper.

The second problem is that the relation between the weightings in the cost function and the achieved imaging quality is not easily determined. In practice, the designer needs to meet a certain performance, i.e. the deformation on the wafer surface needs to be below a certain tolerance. However, tuning the weights in the LQT cost function such that this goal is achieved is not straightforward and will require many iterative designs. It is therefore convenient to

[1] Department of Mechanical Engineering, Eindhoven University of Technology, P.O. Box 513, 5600 MB Eindhoven, The Netherlands
[2] Department of Applied Mathematics, Faculty of Electrical Engineering, Mathematics, and Computer Science, University of Twente, P.O. Box 217, 7500 AE, Enschede, The Netherlands
[3] ASML, De Run 6501, 5504 DR Veldhoven, The Netherlands
Email: d.w.m.veldman@tue.nl, r.h.b.fey@tue.nl, h.j.zwart@tue.nl, marc.van.de.wal@asml.com, joris.van.den.boom@asml.com, h.nijmeijer@tue.nl

formulate the required imaging quality as constraint. This leads to a state-constrained optimization problem and, to the best of our knowledge, actuator design problems have always been studied without state constraints.

In this paper, a method to compute the optimal actuator shape and corresponding (scalar) actuator intensity is presented. The method can deal with input constraints which reflect that thermal actuators can typically only heat or cool and state constraints which guarantee a specified imaging quality. A gradient-based optimization algorithm is used to find the optimal actuator shape and control input simultaneously. The method is applied to a two-dimensional thermomechanical wafer heating model. The obtained actuator shape has a clear physical interpretation.

The remainder of this paper is structured as follows. In Section II, the wafer heating physics are described and the optimal actuator shape design problem is formulated. In Section III, the optimization procedure is discussed. In Section IV, the resulting actuator shapes are presented. Finally, in Section V the conclusions are formulated and discussed.

II. PROBLEM FORMULATION

A. Wafer heating model

A wafer is a silicon disk which typically has a radius of 300 mm and a thickness of 0.7 mm which is placed on a supporting structure. Because the wafer is thin, the temperature variations along the thickness are negligible and the temperature field in the wafer can be considered to be a function of the in-plane Cartesian coordinates (x,y) and time t. Assuming the supporting structure has a constant temperature T_0, the temperature increase in the wafer T is the solution of the two-dimensional heat equation

$$\rho cH\frac{\partial T}{\partial t} = kH\left(\frac{\partial^2 T}{\partial x^2}+\frac{\partial^2 T}{\partial y^2}\right) - h_c T + Q, \qquad (1)$$

where ρ, c, k, and H are the mass density, heat capacity, thermal conductivity, and thickness of the wafer, respectively, h_c models the cooling to the supporting structure, and $Q = Q(x,y,t)$ is the applied heat load that results from the expose light and the thermal actuators, i.e. $Q = Q_{\text{exp}} + Q_{\text{act}}$. The heat load Q_{exp} is induced by the exposing light that projects the pattern of electronic connections on the wafer and has a power P_{exp} [W] which is uniformly applied over the slit $\Omega_{\text{slit}} \subset \mathbb{R}^2$ (the red area in Fig. 1 with length L and width W) which moves with a constant velocity v in the positive y-direction. The actuation heat load Q_{act} will be discussed further in the next subsection. Since the area in which the heat load is applied is small compared to the wafer, the spatial domain $(x,y) \in \mathbb{R}^2$ is considered to be infinite. Time runs from 0 to t_e, where t_e is the time it takes to scan a single field of the wafer which typically contains 100 fields. The wafer temperature is initially equal to T_0, i.e. the initial condition is $T(x,y,0) = 0$.

Because the considered domain is infinite and the applied heat load is moving, it is convenient to consider a moving coordinate system $(x,\zeta,t) = (x,y-vt,t)$ in which the heat load is fixed. In these new coordinates, (1) becomes (see e.g. [13, Chapter 11])

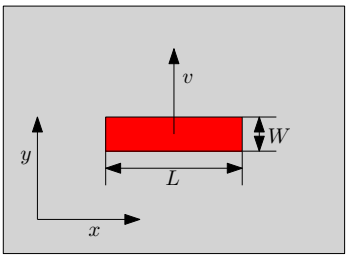

Fig. 1: The heat load (red) that is applied to the wafer (gray)

$$\rho cH\left(\frac{\partial T}{\partial t} - v\frac{\partial T}{\partial \zeta}\right) = kH\left(\frac{\partial^2 T}{\partial x^2}+\frac{\partial^2 T}{\partial \zeta^2}\right) - h_c T + Q. \qquad (2)$$

The mechanical model used to predict the resulting in-plane displacement fields is based on linear strain-displacement relations and the plane-stress relations for an isotropic material. It is assumed that inertia effects are negligible, which is a standard assumption in thermomechanical models (see e.g. [14]). The resulting model in ζ-coordinates takes the form

$$\frac{EH}{1-\nu^2}\left(\frac{\partial^2 d_x}{\partial x^2}+\frac{1-\nu}{2}\frac{\partial^2 d_\zeta}{\partial \zeta^2}+\frac{1+\nu}{2}\frac{\partial^2 d_\zeta}{\partial x \partial \zeta}\right) - k_s d_x = \frac{\alpha EH}{1-\nu}\frac{\partial T}{\partial x}, \qquad (3)$$

$$\frac{EH}{1-\nu^2}\left(\frac{\partial^2 d_\zeta}{\partial \zeta^2}+\frac{1-\nu}{2}\frac{\partial^2 d_x}{\partial x^2}+\frac{1+\nu}{2}\frac{\partial^2 d_x}{\partial x \partial \zeta}\right) - k_s d_\zeta = \frac{\alpha EH}{1-\nu}\frac{\partial T}{\partial \zeta}, \qquad (4)$$

where $d_x = d_x(x,\zeta,t)$ and $d_\zeta = d_\zeta(x,\zeta,t)$ are the displacement fields in x- and ζ-direction, respectively, E, ν, and α are the Young's modulus, Poisson's ratio, and coefficient of thermal expansion of the wafer, respectively, and k_s accounts for the stiffness of the supporting structure. Note that there is a one-sided coupling from the thermal to the mechanical domain.

B. Optimal actuator shape design problem

The actuation heat load Q_{act} has one fixed shape of which the intensity varies over time, i.e.

$$Q_{\text{act}}(x,\zeta,t) = B(x,\zeta)u(t), \qquad (5)$$

where $B(x,\zeta)$ is the actuator shape and $u(t)$ is the intensity. The idea behind (5) is that $B(x,\zeta)$ will indicate where heaters or coolers should be placed. Note that the shape $B(x,\zeta)$ is described in the moving ζ-coordinate system, which means that the designed actuator shapes are fixed to the expose load Q_{exp} and move w.r.t. the wafer. Also note that the representation (B,u) of Q_{act} is clearly nonunique. One easily sees that for example $(-2B,-u/2)$ is a representation of the same actuation heat load $B(x,\zeta)u(t)$. Part of this nonuniqueness is removed by normalizing the actuator shapes $B(x,\zeta)$

to have unit L^1-norm, which means that $B(x,\zeta)$ has unit [1/m^2] so that $u(t)$ has unit [W]. The remaining freedom to scale $B(x,\zeta)$ and $u(t)$ by -1 will be removed below. It should be emphasized that although the representation (B,u) is nonunique, this discussion does not demonstrate that the resulting (single-shape) actuator heat load $B(x,\zeta)u(t)$ is not unique. Whether the single-shape actuator heat load is unique is an open question, which will be discussed more later on.

The goal is to design an optimal actuator shape $B(x,\zeta)$ and the intensity $u(t)$. These should satisfy the following five conditions:

- Since thermal actuators can often only heat or only cool, it is required that the sign of the intensity $u(t)$ does not change over time, which means that the sign of the actuator shape $B(x,\zeta)$ will indicate which locations should be heated and which locations should be cooled and overlap of heaters and coolers is avoided. It is thus required that for all $0 \le t \le t_e$

$$u(t) \ge 0. \tag{6}$$

- For practical reasons, the actuation heat load should not interfere with the projection of patterns on the wafer. Therefore, the actuation heat load cannot be applied in the slit, i.e. for all $(x,\zeta) \in \Omega_{\text{slit}}$

$$B(x,\zeta) = 0. \tag{7}$$

- The applied actuator heat load results in a sufficiently good imaging quality. This is achieved when the deformation in the slit is below a certain threshold δ_{slit}, i.e. for all $(x,\zeta) \in \Omega_{\text{slit}}$ and $0 \le t \le t_e$

$$d_x^2(x,\zeta,t) + d_\zeta^2(x,\zeta,t) < \delta_{\text{slit}}^2. \tag{8}$$

- The actuation heat load prevents slip between the wafer and the supporting structure, which means that the displacements in the whole wafer surface should be below threshold δ_{slip}, i.e. for $(x,\zeta) \in \mathbb{R}^2$ and $0 \le t \le t_e$

$$d_x^2(x,\zeta,t) + d_\zeta^2(x,\zeta,t) < \delta_{\text{slip}}^2. \tag{9}$$

- The applied actuator heat load is minimal, i.e. the actuation heat load has minimal (squared) L^2-norm

$$J_0 = \int_0^{t_e} \iint_{\mathbb{R}^2} Q_{\text{act}}^2(x,\zeta,t)\ \mathrm{d}x\ \mathrm{d}\zeta\ \mathrm{d}t. \tag{10}$$

It will be convenient to write (8) and (9) as one inequality

$$d_x^2(x,\zeta,t) + d_\zeta^2(x,\zeta,t) < \delta_{\text{max}}^2(x,\zeta), \tag{11}$$

where $\delta_{\text{max}}(x,\zeta) = \min\{\delta_{\text{slit}}, \delta_{\text{slip}}\}$ when $(x,\zeta) \in \Omega_{\text{slit}}$ and $\delta_{\text{max}}(x,\zeta) = \delta_{\text{slip}}$ otherwise. The problem is thus to minimize the cost functional J_0 in (10) over all actuator shapes $B(x,\zeta)$ and intensities $u(t)$ subject to (6), (7), and (11).

III. OPTIMIZATION PROCEDURE

Finding a solution to the optimization problem formulated in the previous section is not trivial, particularly because of the nonlinear state constraint on the resulting displacements in (11). Therefore a two-step optimization procedure is proposed in which two considerably simpler optimization problems that only involve linear input constraints need to be solved. In the first step, it is attempted to find an actuator shape $B(x,\zeta)$ and intensity for which the constraints (6), (7), and (11) are satisfied. Note that depending on the values of δ_{slit} and δ_{slip} such a solution might not exist and that it is not trivial to find such a solution. In the second step, the admissible solution found in the first step is used as a starting point for the minimization of the cost functional J_0 in (10) subject to the constraints (6), (7), and (11).

A. Finding an admissible solution

To find an admissible solution, the minimization of the following cost functional is considered

$$J_1 = \int_0^{t_e} \iint_{\mathbb{R}^2} \left[d_x^2(x,\zeta,t) + d_\zeta^2(x,\zeta,t) - \delta_{\text{max}}^2(x,\zeta) \right]^+ \mathrm{d}x\ \mathrm{d}\zeta\ \mathrm{d}t, \tag{12}$$

where the function $[\cdot]^+ : \mathbb{R} \to \mathbb{R}$ is defined by

$$[a]^+ = \begin{cases} a & \text{when } a \ge 0, \\ 0 & \text{otherwise.} \end{cases} \tag{13}$$

Note that the integrand only contributes to the value of J_1 when $d_x^2(x,\zeta,t) + d_\zeta^2(x,\zeta,t) - \delta_{\text{max}}^2(x,\zeta) > 0$, so when the maximally allowed displacement is exceeded. Furthermore, note that $J_1 \ge 0$ and that $J_1 = 0$ implies that the maximally allowed displacement $\delta_{\text{max}}(x,\zeta)$ is not exceeded. Finally, note that J_1 is convex (but not strictly convex) in the displacement fields d_x and d_ζ, and by linearity of (2)–(4) also convex in the applied heat load Q_{act}.

An admissible solution $J_1 = 0$ can thus be found by minimizing J_1 subject to the constraints (6) and (7). In general, a solution resulting in $J_1 = 0$ is not unique. When a minimum where $J_1 > 0$ is found the situation is more involved. Without the requirement that the applied heat load Q_{act} consists of a single actuator shape (see (5)), the convexity of J_1 in Q_{act} implies that the value of local minimum is unique (see e.g. [15]) so it is guaranteed that no admissible solution exists. However, with the actuation heat load of the form (5) it has not been proven that no admissible solution exists.

B. Finding the optimal solution

As already mentioned, the admissible solution found by the procedure from the previous subsection is clearly nonunique and will typically not be the solution with minimal L^2-norm in (10) as is required. A barrier functional J_2 is used to assure that the constraint (11) remains satisfied during the optimization process. The barrier functional is defined as $J_2 = \infty$ when the constraint (11) is not satisfied for any $(x,\zeta) \in \mathbb{R}^2$ and $0 \le t \le t_e$ and otherwise as

$$J_2 = \int_0^{t_e} \iint_{\mathbb{R}^2} \left(\frac{\delta_{\text{max}}^2(x,\zeta)}{\delta_{\text{max}}^2(x,\zeta) - d_x^2(x,\zeta,t) - d_\zeta^2(x,\zeta,t)} \right)^p \mathrm{d}x\ \mathrm{d}\zeta\ \mathrm{d}t, \tag{14}$$

where the power $p > 1$ should be chosen such that points (x,ζ,t) for which the margin in (11) is small affect the value of J_2 significantly more than points for which the margin in

(11) is large. In particular, the value $p = 3$ used in Section IV assures that points for which the margin in (11) is below 4% contribute a 1000 times more than points for which the margin in (11) is larger than 50%. Now consider

$$J_0 + wJ_2, \tag{15}$$

where $w > 0$ is a weight that is chosen such that J_0 and wJ_2 are of similar magnitude. Minimizing (15) subject to the constraints (6) and (7) yields a solution to the optimal actuator shape design problem.

Note that J_2 is convex in Q_{act}, so that the cost functional $J_0 + wJ_2$ is strictly convex in Q_{act} which means that without the requirement that Q_{act} consists of a single actuator shape the optimized actuation heat load is unique (see e.g. [15]). Furthermore, it follows that minimizing $J_0 + wJ_2$ for a fixed actuator shape $B(x,\zeta)$ yields a unique optimal intensity $u(t)$ and minimizing $J_0 + wJ_2$ for a fixed intensity $u(t)$ yields a unique actuator shape $B(x,\zeta)$. Uniqueness of the single-shape actuator heat load $B(x,\zeta)u(t)$ has not been proven. However, it has been observed for several design problems that different starting points and different optimization algorithms all converge to the same applied heat load $B(x,\zeta)u(t)$, which suggests that the optimal actuator shape is in fact unique (at least for the considered wafer heating problem).

C. Optimization algorithm

To use the method from the previous two subsections, two optimization problems with a convex cost functional $J = J(B,u)$ and linear input constraints need to be solved. Such problems are typically solved by gradient-based optimization (see e.g. [15]). Note however that in both cases the optimization runs over two unknowns, the actuator shape $B(x,\zeta)$ and the intensity $u(t)$, that appear as a product. Because of this unusual form the optimization program was coded in MATLAB and no existing software was used.

First, the temperature field $T(x,\zeta,t)$, the displacement fields $d_x(x,\zeta,t)$ and $d_\zeta(x,\zeta,t)$, and the actuator shape $B(x,\zeta)$ are expressed in terms of FE shape functions. The Galerkin method then leads to the spatial discretization of the governing equations (2)–(4) and the cost functionals in (10), (12), and (14). For the numerical integration over time a fixed step size fourth-order Runge-Kutta solver is used. For both optimization problems formulated in the previous subsections, the sensitivities $\nabla_B J(B,u)$ and $\nabla_u J(B,u)$ are computed using adjoint states (see e.g. [16] or [17]).

In both minimization problems, the actuator shape and intensity are updated alternately by the projected gradient method (see e.g. [17] or [18]). For example, the next iterate for the actuator shape $B^{(i+1)} = B^{(i+1)}(x,\zeta)$ is computed as

$$B^{(i+1)} = \Pi_B \left(B^{(i)} - h_B \nabla_B J(B^{(i)}, u^{(i)}) \right), \tag{16}$$

where Π_B is the projection on the set of actuator shapes that satisfy (7), $u^{(i)} = u^{(i)}(t)$ is the i-th iterate of the control input, and $h_B > 0$ is the step size that is determined based on a second-order Taylor series expansion

$$J(B^{(i+1)}, u^{(i)}) \approx J(B^{(i)}, u^{(i)}) + G_B^{(i)} h_B + \frac{1}{2} H_B^{(i)} h_B^2, \tag{17}$$

where $G_B^{(i)} < 0$ and $H_B^{(i)} > 0$ contain the gradient and Hessian information, respectively. Starting from $h_B = -G_B^{(i)} / H_B^{(i)}$, h_B is halved until $J(B^{(i+1)}, u^{(i)}) < J(B^{(i)}, u^{(i)})$. After that, the intensity $u^{(i)}$ is updated in the direction $-\nabla_u J(B^{(i+1)}, u^{(i)})$ by a similar procedure. The convergence criterion is that the relative changes in cost functional J, actuator shape B, and intensity u should all be below a tolerance `tol` after both B and u have been updated.

It should be noted that the actuator shape $B(x,\zeta)$ is not enforced to have unit L^1-norm during the update process because allowing this scaling freedom does not result in conditioning problems since either the actuator shape $B(x,\zeta)$ or the intensity $u(t)$ is fixed during every update step. The normalization $\|B\|_{L^1} = 1$ can easily be achieved after the optimum has been found by rescaling $B(x,\zeta)$ and $u(t)$.

IV. RESULTS

To construct the FE model, the infinite domain $(x,\zeta) \in \mathbb{R}^2$ is truncated to $(x,\zeta) \in [-2L, 2L] \times [-3vt_e, 2vt_e]$, which is chosen such that the temperature increase at the edges of the domain is negligible. The FE model uses linear quadrilateral elements and has 1323 nodes, of which 252 are located inside the slit so that the actuator shape $B(x,\zeta)$ is described by 1071 nodal values. The time interval $[0, t_e]$ is discretized using 100 uniformly distributed time points.

The used parameter values are given in Table I. Note that an actuation heat load will be designed that achieves a maximal deformation in the slit of $\delta_{\text{slit}} = 2$ nm, which is a reduction of a factor 2 compared to the maximal deformation of 4.1 nm that occurs without actuation. Also observe that $\delta_{\text{slip}} = 3.67$ nm is exceeded without actuation, which means actuation is needed to prevent slip.

Fig. 2 illustrates the design procedure described in the previous section. Starting from the initial guess in Fig. 2(a) where the actuator shape $B(x,\zeta) = 0$ and the intensity is $u(t) = 10^5$ [W], minimizing J_1 in (12) leads to the admissible design in Fig. 2(b). This design is then used to initialize the optimization procedure for $J_0 + wJ_2$, which leads to the design in Fig. 2(c). Note that the normalization $\|B\|_{L^1} = 1$ is applied in Figs. 2 and 3, unless $B(x,\zeta) = 0$.

The designed optimal actuator shape in Fig. 2(c) can be explained by our physical understanding of the wafer heating problem. The actuator shape $B(x,\zeta)$ shows that the cooling is applied around the slit. Note that having $Q_{\text{act}} = -Q_{\text{exp}}$ would result in zero deformations because no net heat load is applied. However, the constraint (7) excludes this solution. The cooling around the slit in Fig. 2(c) attempts to have some of this effect while respecting the constraint (7). A more surprising aspect of the shape in Fig. 2(c) is the heating applied in the area where $\zeta > 0$. To understand this, recall that the expose load moves in the positive y-direction, which means that during the scanning of the field the heat applied by the expose light is accumulating behind the heat load, so in the area where $\zeta < 0$. The thermal expansion due to this heating pushes the slit in the positive ζ- (or y-)direction. The actuation heat load applied in the area where $\zeta > 0$ now creates thermal expansion in front of the slit, which pushes

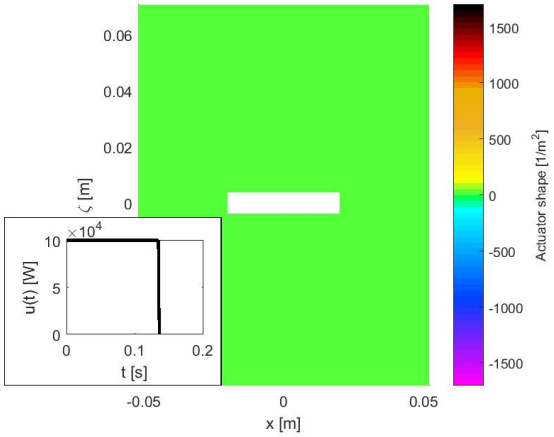

(a) Initial guess

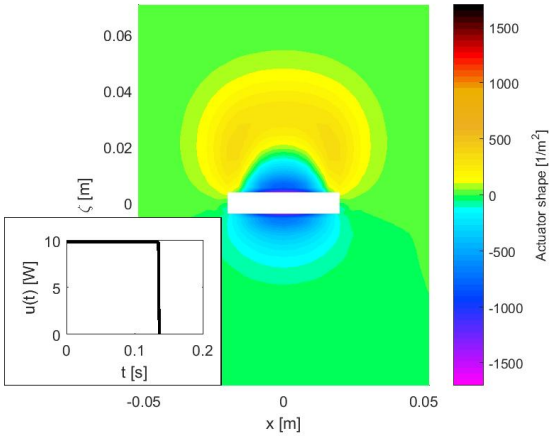

(b) Admissible design

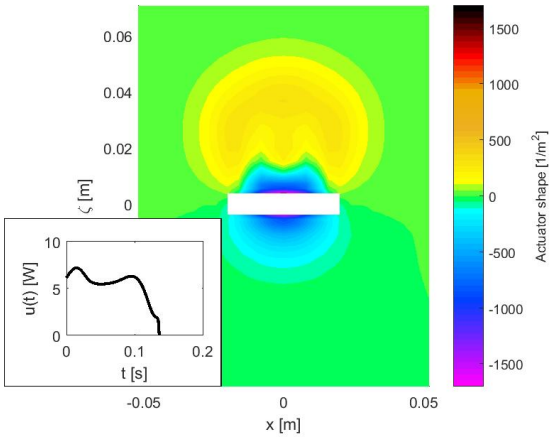

(c) Optimal design

Fig. 2: Actuator shapes $B(x,\zeta)$ and intensities $u(t)$ that are used as initial guess in the optimization (a), that are obtained after searching for an admissible solution (b), and that are obtained after minimizing the actuation effort (c). The white area in the center of the actuator shape is the slit Ω_{slit} in which actuation is not possible.

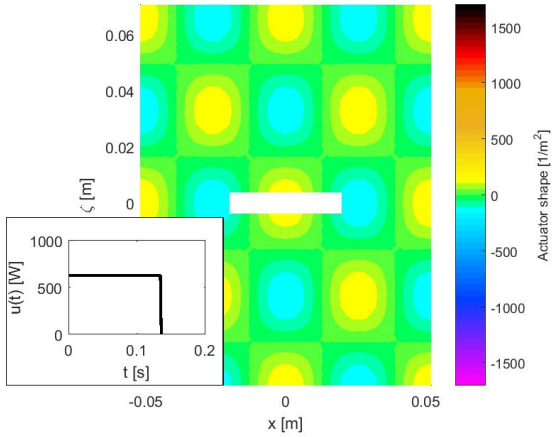

(a) Initial guess

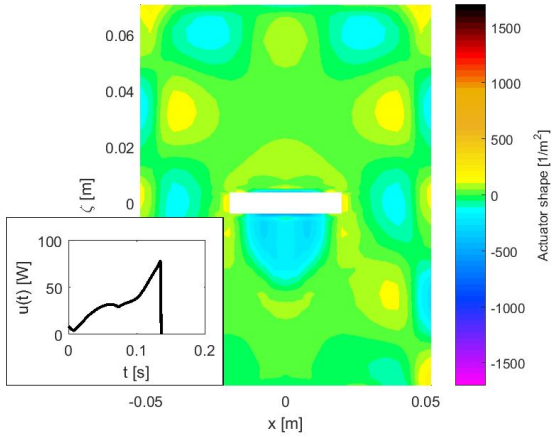

(b) Admissible design

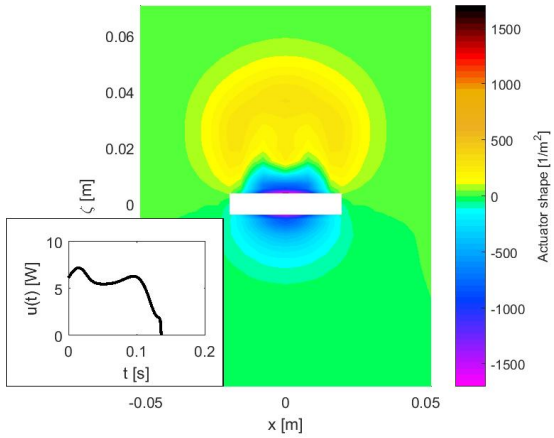

(c) Optimal design

Fig. 3: Actuator shapes $B(x,\zeta)$ and intensities $u(t)$ that are used as initial guess in the optimization (a), that are obtained after searching for an admissible solution (b), and that are obtained after minimizing the actuation effort (c). The white area in the center of the actuator shape is the slit Ω_{slit} in which actuation is not possible.

TABLE I: Parameter values

ρ	2329 [kg/m^3]	E	167 [GPa]
c	705 [J/kg·K]	ν	0.3 [-]
H	0.775 [mm]	k_s	1.21 $\cdot 10^{12}$ [N/m^3]
k	149 [W/K·m]	δ_{slit}	2 [nm]
h_c	1500 [W/m$^2\cdot$ K]	δ_{slip}	3.67 [nm]
P_{exp}	3.2 [W]	p	3 [-]
L	26 [mm]	w	10^5 [W^2/m^4]
W	4.6 [mm]	`tol`	10^{-5} [-]
t_e	0.136 [s]		

the slit back in the negative ζ- (or y-)direction, thus reducing the total deformation that will be observed in the slit.

Fig. 3 shows the designed actuator shapes $B(x,\zeta)$ and intensities $u(t)$ that are obtained when the initial actuator shape is chosen as $B(x,\zeta) = \cos(\pi x/L)\cos(\pi\zeta/(vt_e))$ [1/m^2] and the initial intensity as $u(t) = 10^5$ [W] (note that this initial guess does not satisfy $\|B\|_{L^1} = 1$ and is rescaled in Fig. 3(a)). When comparing the results in Figs. 2 and 3, it is clear that the obtained admissible solutions in subfigures (b) are different but that the optimal solutions in subfigures (c) look very similar. The fact that the actuator shapes and intensities are different in subfigures (b) illustrates that there are indeed many admissible solutions that satisfy the constraints (6), (7), and (11) and the particular solution that is found after minimizing J_1 depends on the initial guess that is used. This is also reflected by the fact that J_1 is not a strictly convex function in the applied actuator heat load Q_{act}, which indicates the minimizer is not unique. It is remarkable that the optimal designs in subfigures (c) are very similar. This suggests that the single-actuator shape solution might be unique for the considered problem, but at the moment there is no theoretical support for this claim.

Actuator shape designs for the considered FE model with 1323 nodes can be made conveniently on a normal laptop. The running times will obviously depend on the initial guess. The results in Fig. 2(b) were obtained after one update of the actuator shape $B(x,\zeta)$ which took 5s. Obtaining the optimized actuator shape in Fig. 2(c) required 393 updates of $B(x,\zeta)$ and $u(t)$ which took about 32 minutes. Starting from the initial guess in Fig. 3(a) 8 updates of $B(x,\zeta)$ and $u(t)$ (which took 41s) were needed to obtain the profile in Fig. 3(b) and 577 updates of $B(x,\zeta)$ and $u(t)$ (which took 43 minutes) were needed to obtain the profile in Fig. 3(c).

V. CONCLUSIONS AND DISCUSSIONS

An approach to design optimal actuator shapes and corresponding intensities for the wafer heating problem has been proposed. The method has been demonstrated to design optimal actuator shapes for the scanning of a single field on a wafer for a model in two spatial dimensions.

It should be noted that the method has great flexibility and can be applied to many variations of the problem considered in this paper that are relevant for the design of an actuator layout. For example, it is easy to extend the presented method to design actuator shapes that can only heat (i.e. add the constraint $B(x,\zeta) \geq 0$) or actuator shapes that can only cool (i.e. add the constraint $B(x,\zeta) \leq 0$). By reformulating the FE model it is also possible to consider fields near the edge of the wafer and the scanning of multiple fields.

As noted before, the uniqueness of the single-shape actuator heat load $B(x,\zeta)u(t)$ has not been proven. However, the numerical results in Section IV seem to indicate that the algorithm always converges to the same applied actuator heat load $B(x,\zeta)u(t)$. A proof of such claim seems challenging because the structure of the problem is similar to a (constrained) low-rank approximation problem (see e.g. [19]). The understanding of such problem is currently rather limited compared to the well-known unweighted low-rank approximation problem.

Note that the proposed design does not take into account uncertainties such as the reflection of the wafer and the cooling rate to the supporting structure (h_c in (1) and (2)). We intend to design a feedback control system that can compensate for such uncertainties in a future work.

REFERENCES

[1] L. Subramany, W. J. Chung, P. Samudrala, H. Gao, N. Aung, J. M. Gomez, B. Minghetti, and S. Lee, "Analysis of wafer heating in 14nm DUV layers," in *Metrology, Inspection, and Process Control for Microlithography XXX*. International Society for Optics and Photonics, 2016.

[2] N. Aung, W. J. Chung, P. Samudrala, H. Gao, W. Gao, D. Brown, G. He, B. Park, M. Hsieh, X. Hao, *et al.*, "Overlay control for 7nm technology node and beyond," in *Optical Microlithography XXXI*. International Society for Optics and Photonics, 2018.

[3] D. van den Hurk, S. Weiland, and K. van Berkel, "Modeling and localized feedforward control of thermal deformations induced by a moving heat load," in *SICE International Symposium on Control Systems*, 2018.

[4] S. Skogestad and I. Postlethwaite, *Multivariable feedback control: analysis and design*. Wiley New York, 2007, vol. 2.

[5] M. van de Wal and B. de Jager, "A review of methods for input/output selection," *Automatica*, vol. 37, no. 4, pp. 487–510, 2001.

[6] F. Al-Sulaiman and S. Zaman, "Actuator placement in lumped parameter systems subjected to disturbance," *Computers & structures*, vol. 52, no. 1, pp. 41–47, 1994.

[7] Y. Cao, D. Biss, and J. Perkins, "Assessment of input-output controllability in the presence of control constraints," *Computers & chemical engineering*, vol. 20, no. 4, pp. 337–346, 1996.

[8] D. S. Naidu, *Optimal control systems*. CRC press, 2002.

[9] A.-C. Boulanger and P. Trautmann, "Sparse optimal control of the kdv-burgers equation on a bounded domain," *SIAM Journal on Control and Optimization*, vol. 55, no. 6, pp. 3673–3706, 2017.

[10] Y. Privat, E. Trélat, and E. Zuazua, "Actuator design for parabolic distributed parameter systems with the moment method," *SIAM Journal on Control and Optimization*, vol. 55, no. 2, pp. 1128–1152, 2017.

[11] D. Kalise, K. Kunisch, and K. Sturm, "Optimal actuator design based on shape calculus," *arXiv preprint arXiv:1711.01183*, 2017.

[12] D. R. Herber and J. T. Allison, "Nested and simultaneous solution strategies for general combined plant and control design problems," *Journal of Mechanical Design*, vol. 141, no. 1, p. 011402, 2019.

[13] D. W. Hahn and M. N. Özişik, *Heat conduction*, 3rd ed. John Wiley & Sons, 2012.

[14] Y.-c. Fung, P. Tong, and X. Chen, *Classical and computational solid mechanics*. World Scientific, 2001, vol. 1.

[15] S. Boyd and L. Vandenberghe, *Convex optimization*. Cambridge university press, 2004.

[16] E. B. Lee and L. Markus, *Foundations of optimal control theory*. John Wiley & Sons, 1967.

[17] A. Borzì and V. Schulz, *Computational optimization of systems governed by partial differential equations*. SIAM, 2011, vol. 8.

[18] M. Ulbrich, *Optimization Methods in Banach Spaces*. Springer, 2009, pp. 97–156.

[19] J. H. Manton, R. Mahony, and Y. Hua, "The geometry of weighted low-rank approximations," *IEEE Transactions on Signal Processing*, vol. 51, no. 2, pp. 500–514, 2003.